Mitochondrial cristae remodelling is associated with disrupted OPA1 oligomerisation in the Huntington's disease R6/2 fragment model

Tanja Hering[a], Kerstin Kojer[a], Nathalie Birth[a], Jaqueline Hallitsch[a], Jan-Willem Taanman[b], Michael Orth[a*]

[a]Department of Neurology, Ulm University, Germany

[b]Department of Clinical Neurosciences, Institute of Neurology, University College London, London, UK

* Corresponding author: Michael Orth, MD PhD

Department of Neurology

Ulm University

Oberer Eselsberg 45/1, 89081 Ulm, Germany

e-mail: michael.orth@uni-ulm.de

Tel: +49-731 50063095; Fax: +49-731 50063082

Highlights

- In striatum and cortex of R6/2 mice, mitochondrial cristae morphology was abnormal
- Levels of the fission and fusion factors, and mitofilin protein assemblies, were unaffected
- OPA1 oligomerisation was decreased in striatum and cortex of transgenic mice
- Mutant huntingtin may impair OPA1 oligomerisation and cristae integrity

Abstract

There is evidence of an imbalance of mitochondrial fission and fusion in patients with Huntington's disease (HD) and HD animal models. Fission and fusion are important for mitochondrial homeostasis including mitochondrial DNA (mtDNA) maintenance and may be relevant for the selective striatal mtDNA depletion that we observed in the R6/2 fragment HD mouse model. We aimed to investigate the fission/fusion balance and the integrity of the mitochondrial membrane system in cortex and striatum of end-stage R6/2 mice and wild-type animals. Mitochondrial morphology was determined using electron microscopy, and transcript and protein levels of factors that play a key role in fission and fusion, including DRP1, mitofusin 1 and 2, mitofilin and OPA1, and cytochrome c and caspase 3 were assessed by RT-qPCR and immunoblotting. OPA1 oligomerisation and mitofilin protein associations were evaluated using blue native gels. In striatum and cortex of R6/2 mice, mitochondrial cristae morphology was abnormal. Although the overall levels of the fission and fusion factors were unaffected, OPA1 oligomerisation was decreased in striatum and cortex of R6/2 mice. Mitochondrial and cytoplasmic cytochrome c levels were similar R6/2 and wild-type mic without a significant increase of activated caspase 3. Our results indicate that the integrity of the mitochondrial cristae is compromised in striatum and cortex of the R6/2 mice and that this is most likely caused by impaired OPA1 oligomerisation.

Keywords: OPA 1 oligomerisation; cristae integrity; fission and fusion; mitofilin; caspase 3

Introduction

Huntington`s disease (HD) is a fatal neurodegenerative disease, caused by a CAG repeat expansion mutation in exon 1 of the huntingtin gene (*HTT*) (The Huntington's Disease Collaborative Research Group 1993). HD is characterised by a mixed movement disorder, dementia and behavioural problems (Ross and Tabrizi 2011, Ross et al. 2014). While there is good evidence to suggest mitochondrial involvement in HD patients and genetic HD animal models (Bossy-Wetzel et al., 2008; Browne, 2008; Oliveira, 2010; Quintanilla and Johnson, 2009; Reddy et al., 2009), it remains less clear which role mitochondria actually play in the pathogenesis of HD. In addition to mitochondrial involvement in the pathogenesis of HD, we have shown in wild-type mice that the striatum and cortex exhibit inherent differences in potentially important aspects of mitochondrial biology and that these differences may contribute to the increased vulnerability of the striatum to the pathogenic events in HD (Hering et al. 2015).

Much interest was focused recently on the fission/fusion balance in HD. Mutant huntingtin (mHTT) was shown to interact with the main driver of mitochondrial fission, the GTPase dynamin related protein 1 (DRP1), with increased DRP1 activity associated with increased fragmentation of the mitochondrial network in human HD fibroblast and lymphoblast cell cultures as well as in HD mouse primary neurons and brain (Jin et al. 2013, Shirendeb et al. 2012, Song et al. 2011). In HD patient lymphoblasts and primary striatal neurons derived from YAC128 transgenic mice, DRP1 translocation to mitochondria was associated with increased mitochondrial fragmentation (Costa 2010). In post-mortem HD patient striatum, mitochondria were smaller with an increase in DRP1 protein levels predominantly in late stage HD (Kim et al. 2010) and an increase in enzymatic DRP1 activity (Shirendeb et al. 2012). In HeLa cells expressing mHTT as well as in different HD cells lines, the mitochondrial network was shown to be more fragmented and contain mitochondria with alterations in cristae structure and enhanced apoptosis (Costa 2010, Costa and Scorrano 2012). Further support for a role of increased mitochondrial fission in the pathogenesis of HD comes from the observation that inhibition of DRP1 reverses the phenotype of mitochondrial fragmentation and improves survival in HD mice (Guo et al. 2013).

Mitochondrial fission and fusion contribute to the maintenance of mitochondrial homeostasis that is essential for mitochondrial function, such as ATP production via oxidative phosporylation, mitochondrial DNA (mtDNA) stability, cellular stress responses, mitophagy and apoptosis regulation (Bereiter-Hahn and Voth 1994, Chan 2006a, 2006b, Twing 2008, Westermann 2010, Youle and van der Bliek 2012). Mitochondrial fission is necessary during cell division and, particular in neurons, for mitochondrial trafficking along the axon to the synapse (Lin and Sheng 2015). The translocation of DRP1 from the cytosol to mitochondria initiates the fission process. The mitochondrial fusion process can be separated into fusion of the outer mitochondrial membrane involving mitofusin 1 (MFN1) and mitofusin 2 (MFN2) and fusion of the inner mitochondrial membrane involving optic atrophy protein 1 (OPA1) (reviewed in (Westermann 2010)). In addition, several proteins, including mitofilin, maintain the integrity of the inner mitochondrial membrane system (MINOS) (von der Malsburg et al. 2011, Zerbes et al. 2012a, Zerbes et al. 2012b).

In a previous study we reported lower mtDNA copy number in striatum of end-stage R6/2 mice without evidence of impaired mitochondrial respiratory chain activity, biogenesis or respiratory chain assembly (Hering et al. 2015). Given the important role of fission and fusion in the maintenance of mtDNA and the evidence implicating an imbalance of fission and fusion in various HD models and HD patient brains, we investigated the fission/fusion balance and the integrity of the mitochondrial membrane systems in striatum and cortex of the R6/2 HD fragment mouse model. We hypothesised that striatum and cortex would show an ultra-structural phenotype of increased fission (smaller, fragmented mitochondria) together with an increase in the amount of DRP1 protein associated with mitochondria of transgenic mice, indicating a shift of the fission/fusion balance towards fission.

Material and Methods

Animals

For all experiments R6/2 transgenic mice (B6CBATg(HDexon1)62Gpb/1J) and their corresponding wild-type B6CBAF1/J were purchased from Jackson Laboratory. Genotyping and the CAG repeat

length determination (approximately 160 ± 10) were performed on DNA extracted from tail biopsies (Mangiarini et al. 1996). According to local regulation and EU Directive 2010/63/EU, 12 week old animals were sacrificed by cervical dislocation. Both striata as well as whole cortex, including all layers, were prepared and immediately snap frozen in liquid nitrogen and then stored at -80°C. For electron microscopy mice were perfused twice with PBS, followed by 4 % paraformaldehyde fixation.

Electron microscopy

Directly after fixation small pieces of about 2x2x2 mm^3 from the central portion of the striatum, or from the middle of the cerebral cortex were carefully prepared and immediately fixed in 2.5 % glutaraldehyde. Two ultra-thin sections from different areas were used for electron microscopy. Representative images of both ultra-thin sections per sample were taken with a Jeol 1400 Transmission Electron Microscope (JEOL GmBH). For quantification, five representative images per sample at x12,000 magnification were used. Images were transferred to a tablet-PC (iPad2, Apple) and mitochondria were outlined using the Glow Draw application (The Othernet, LLC © Daniel Cota), followed by quantification using ImageJ software (ImageJ 1.46r, Wayne Rasband, National Institutes of Health, USA). The median of individual results from each of the five images was calculated for mitochondrial area, number, altered cristae structure and total mitochondrial area per image. Data acquisition and all analyses were done blinded to the genotype of the animal.

Quantitative Real-Time-PCR

RNA was isolated using the RNeasyPlus Mini Kit (Qiagen, Germany) followed by 2 µg cDNA synthesis with the iSkript™cDNA Synthesis Kit (Bio-Rad Laboratories, Germany). For the quantitative PCR reactions, striatum and cortex cDNA and water as negative control were tested in triplicates in a 96 well plate. The PCR reaction was performed using SYBR® green supermix (Bio-Rad Laboratories) and primer pairs against the following genes of interest: *Mfn1* (mitofusin1), *Mfn2* (mitofusin2), *Drp1* (dynamin 1-like protein), *Opa1* (optic atrophy 1), *Immt* (inner membrane protein, mitochondrial),

Cycs (cytochrome c) (for primer sequences see Table 1). *Poldip3* (polymerase (DNA-directed), delta interacting protein 3) and *Metap1* (methionylaminopeptidase 1) were used as reference genes, which had homogenous stable cDNA levels (Mean CV 0.1626 and Mean M Value 0.4761) according to (Hellemans et al. 2007). All reactions were performed with the CFX384 Touch Real-Time PCR Detection Systems (Bio-Rad Laboratories) with the following programme: 95°C for 3 min, followed by 40 cycles of 95°C for 15 sec and a primer-dependent annealing/extension temperature (see Table 1) for 15 sec, and finally a 60-95°C melting curve at increments of 1°C every 5 sec.

Protein extraction, gel electrophoresis and western blot

For western blots of native and denatured proteins, total lysates were prepared from striatum or cortex in homogenisation buffer containing 320 mM sucrose, 1 mM K^+ EDTA, 10 mM Tris/HCl, pH 7.4 and protease inhibitors (1 µg/ml of pepstatin, 1 µg/ml of leupeptin and 1 mM PMSF) and homogenised with Tissue Lyser for 2 min at 50 Hz followed by centrifugation at 600×g for 10 min at 4°C. For the subcellular fractionation of mitochondria and cytoplasm, the striatum (striata pooled from four mice) or the cortex were homogenised on ice in 200 µl homogenisation buffer (see above) with a douncer homogeniser. Lysates were centrifuged at 1300 g for 10 min at 4°C. Supernatant was collected and stored on ice, while the pellet was re-suspended in 200 µl homogenisation buffer, followed by centrifugation as before. Collected supernatant was centrifuged at 17.000 x g for 15 min at 4 °C. The supernatant represents the cytoplasmic fraction and the pellet contains the enriched mitochondrial fraction and was re-suspended in 30 µl homogenisation buffer. Total lysates were snap frozen and thawed three times to break mitochondrial membranes.

For SDS-PAGE and western blot 12 % or 9 % Bis-Tris-gels were used. For protein level analysis 15 µg of total protein extract and for purity analyses of the subcellular fractionations 5 µg protein lysate were used. For analyses of the subcellular fractions 2.5 µg of mitochondria and 15 µg of the cytoplasmic fraction were loaded onto a gel. Native protein analyses were performed with 10 µg total lysate (Schagger and von Jagow 1991). After electrophoresis gels were blotted on PVDF

membranes (Immobilon-P, pore size 0.45 µm, Millipore) followed by total protein stain determination using Pierce Reversible Protein Stain Kit for PVDF Membranes (Pierce, Rockford, USA). Membranes were blocked in 10% non-fat milkpowder solution for 1 h, followed by primary antibody incubation overnight (anti-caspase 3, 9665 Cell Signaling, 1:1000; anti-cytochrome c, BD 556433, 1:1000; anti-DRP1, BD 611112, 1:1000; anti-mitofilin, ab93323 Abcam, 1:1000; anti-mitofusin1, ab126575 Abcam, 1:500; anti-mitofusin2, ab50838 Abcam, 1:1000; anti-OPA1, BD 612606, 1:1000; anti-NDUFA9, ab14713 Abcam, 1:1000; anti-HPRT ab109021 Abcam 1:10000). Following three washing steps with PBS-T (PBS with 0.3 % Tween), membranes were incubated with secondary antibody (goat anti-mouse IgG (H+L)-HPR (1:3000, Bio-Rad) or goat anti-rabbit IgG (H+L) (1:10,000, 111-035-003, Jackson ImmunoResearch)) for 1 h. All antibodies were diluted with 10% milk-PBS-T solution. Following three washing steps with PBS-T we used Image Quant LAS4000 according to the manufacturer's instructions (GE Healthcare Life Science, Freiburg) for specific protein detection. Densitometry results were quantified using Image Quant software and calculated relative to total protein stain, which also allows the direct comparison between striatum and cortex samples. For total protein determination densitometry was performed for each lane loaded with 12.5 µg of protein using Image Quant software. From the mean grey values of immunoblot signals the background signal intensity was subtracted resulting in a single value for each lane. The Complex I subunit NDUFA9 was used as mitochondrial marker protein in mitochondrial fractions and HPRT was used as cytoplasmic marker in cytoplasmic fractions.

Data analysis and statistics

All experiments and data analyses were conducted blinded to the animals' genotype. After decoding data were examined for normal distribution using the Kolmogorov-Smirnov test. Skewed data with non-normal distribution were multiplied by a factor of 10 or 100 to obtain values of more than 1, which is necessary for the log transformation of the data sets leading to normal distribution (Altman 1991).

Normally distributed data were analysed using univariate analysis of variance (ANOVA *F*-test) with the result of the experiment as dependent variable and 'region' and 'genotype' as independent variables. A main effect of 'region' indicated differences between striatum and cortex, while a main effect of 'genotype' indicated a difference between wild-type and transgenic mice and an interaction of region-genotype differences in the regional patterns between wild-type and transgenic animals. Post-hoc analysis were performed with statistical significant level set to p=0.05 with Bonferroni correction for multiple pairwise comparisons. The comparison of two data sets was performed by using Student's t-test. For non-normally distributed skewed data sets we used the Kruskal-Wallis-Test followed by Dunn`s Multiple Comparison test. All statistical analysis was performed with GraphPad Prism 5.

Results

Mitochondrial morphology

Using electron microscopy we determined mitochondrial morphology, including mitochondrial size, number, total mitochondria area and cristae structure in striatum and cortex of 10 transgenic and 10 wild-type mice. Mitochondrial size and number per image as well as the average mitochondrial area per image was similar in R6/2 and wild-type tissues (Figure 1A-D); however, we noticed a marked increase of mitochondria with disorganised cristae. The mitochondria contained fewer cristae, and the cristae were arranged in a non-parallel manner. In addition, some mitochondria appeared to harbour vacuoles. We quantified the number of mitochondria with altered cristae structure and calculated the ratio of abnormal mitochondria to the total number of mitochondria. In striatum and cortex of R6/2 mice the overall proportion of mitochondria with altered cristae structure was increased significantly compared to wild-type tissues (Figure 1A and E, main effect of genotype, $F1.36 = 6.909$, $p = 0.0125$). The difference in abnormal mitochondria was particularly pronounced in the striatum of transgenic mice (17.93 % ± 3.39 SEM versus 6.8 % ± 2.06 SEM in controls, $p < 0.05$; Figure 1D).

Mitochondrial fission/fusion balance

Alterations in the mitochondrial cristae structure could be caused by changes in the mitochondrial fission/fusion balance (Anand et al. 2014, Kushnareva et al. 2013). In R6/2 mice striatum and cortex, mRNA levels of the main fission driver *Drp1* were lower compared to wild-type tissues (main effect of genotype, $F_{1.36} = 5.05$, $p = 0.0309$; Figure 2A). This effect was mainly produced by the lower amount of *Drp1* in cortex of transgenic mice (t-test $p<0.001$). At the protein level the amount of DRP1 was also reduced in cortex of the transgenic mice compared to wild-type (interaction genotype*brain region, $F_{1.39} = 5.04$, $p = 0.0305$; Figure 2B, D). Mitochondrial fission is mainly initiated by the recruitment of cytosolic DRP1 to the outer mitochondrial membrane (Otera et al. 2013). Despite the lower DRP1 levels in total lysate in cortex of transgenic mice, the amount of recruited DRP1 in mitochondrial fractions was similar in cortex and striatal samples of transgenic and wild-type mice (Figure 2 C, D).

We next assessed the mitochondrial outer membrane fusion factors MFN1 and MFN2. At the mRNA level, the amount of *Mfn1* (main effect of brain region, $F_{1.38} = 35.95$, $p < 0.001$; Figure 2E) and *Mfn2* (main effect of brain region, $F_{1.37} = 16.84$, $p = 0.002$; Figure 2F) were lower in wild-type cortex than in striatum. At the protein level, MFN2 (main effect of brain region, $F_{1.38} = 8.41$, $p = 0.0062$; Figure 2 H and I) was also lower in wild-type cortex compared to striatum. In transgenic mice only the mRNA levels of *Mfn1* in striatum were higher compared to wild-type (interaction genotype*brain region, $F_{1.38} = 7.93$, $p = 0.0077$; transgenic versus wild-type striatum $p < 0.01$; Figure 2E).

Cristae structure proteins

We next examined factors that contribute to the control and maintenance of the mitochondrial cristae structure. First, we assessed mitofilin, an important member of the mitochondrial inner membrane organising system (MINOS) (Zerbes et al. 2012a). Mitofilin mRNA (*Immt*) levels, and levels of both the denatured mitofilin (IMMT) and native mitofilin protein assemblies were similar in wild-type striatum and cortex as well as in transgenic and wild-type mice (Figure 3A, B, C, D).

Fusion of the mitochondrial inner membrane is mainly regulated by OPA1. In addition, OPA1 is also crucial for cristae stability. *Opa1* mRNA levels in wild-type cortex were lower than in the striatum (main effect of brain region, $F_{1.38} = 34.54$, $p < 0.0001$; Figure 4A), and lower in transgenic mice than in wild-type (main effect of genotype, $F_{1.38} = 7.73$, $p = 0.008$; Figure 4A). The pattern of *Opa1* mRNA levels differed between transgenic and wild-type mice (interaction genotype*brain region, $F_{1.38} = 7.73$, $p = 0.008$). In cortex of transgenic mice the amount of *Opa1* mRNA was lower than in wild-type, while in striatum the amount of *Opa1* mRNA was similar in wild-type and transgenic mice (transgenic versus wild-type cortex $p < 0.001$; Figure 4A).

The OPA1 precursor protein can be separated into the long membrane anchored isoform and the short cleaved soluble isoform. Both isoforms are present in healthy mitochondria and are necessary for efficient fusion (Anand et al. 2014). In wild-type and transgenic mice, the protein levels of the long OPA1 isoform relative to the short isoform were lower in cortex compared to striatum (main effect of brain region, $F_{1.32} = 16.26$, $p = 0.0003$; Figure 4B, C). In the cortex of transgenic mice OPA1 levels of the short (main effect of genotype, $F_{1.35} = 5.12$, $p = 0.03$, transgenic versus wild-type cortex $p < 0.05$; Figure 4C, Figure S1A) and long isoforms (transgenic versus wild-type cortex $p < 0.05$; Figure 4C, Figure S1B) were lower than in wild-type, with a lower ratio of long relative to short isoform (interaction genotype*brain region, $F_{1.32} = 4.58$, $p = 0.0401$, transgenic versus wild-type cortex posttest $p < 0.05$; Figure 4B, C). In addition to the cleavage of OPA1 during e.g. mitophagy and apoptosis, decreased OPA1 oligomerisation can lead to opening of cristae junctions during apoptosis (Frezza et al. 2006; Yamaguchi et al. 2008). OPA1 oligomer determination using blue native gel electrophoreses and western blot revealed three discernible bands at about 1200, 500 and 300 kDa (Figure 4F). In transgenic mice the amount of the high molecular weight oligomers at 1200 kDa was slightly reduced (Figure 4D, F), while the amount of the lowest molecular weight at 300 kDa was increased (main effect of genotype, $F_{1.34} = 5.71$, $p = 0.0225$, Figure 4E, F). The difference was particularly prominent in the striatum (transgenic versus wild-type striatum $p < 0.05$; Figure 4E, F).

Cytochrome c and caspase 3

The ultra-structural abnormalities of cristae morphology and the lower amount of low molecular weight OPA1 oligomers in our mice could be associated with impaired mitochondrial membrane integrity (Frezza et al. 2006). Downregulation of OPA1 can lead to vacuolar cristae (Olichon et al. 2003) and wider cristae structure (Frezza et al. 2006), which has been shown to be associated with apoptosis. A link between impaired cristae structure and apoptosis could be the release of cytochrome c from mitochondria into the cytoplasm. We therefore next asked if there was a shift from mitochondrial to cytosolic cytochrome c indicative of the release of cytochrome c from mitochondria into the cytosol. The total amount of cytochrome c, at mRNA level (main effect of brain region, $F1.32 = 11.15$, $p = 0.0021$; Figures S2A) and protein level (main effect of brain region, $F1.33 = 35.18$, $p < 0.0001$; Figures S2B) was lower in wild-type cortex than striatum. The amount of cytochrome c was determined in mitochondria and the corresponding cytosol after tissue fractionation (Figure 5A). Levels of cytochrome c in mitochondria and cytosol were similar in transgenic and wild-type mice (Figure 5B). Release of cytochrome c from mitochondria into the cytosol could trigger cleavage of caspase 3 and subsequent induction of apoptosis. Levels of the cleaved active caspase 3 were slightly higher in transgenic mice (main effect of genotype, $F1.25 = 3.33$, $p=0.08$; Figure S2C,F), even though the difference did not quite reach statistical significance. This is consistent with the ratios of cleaved to uncleaved caspase 3, which were similar in transgenic and wild-type mice (Figure S2D).

Discussion

In this study we show that in the striatum and cortex of the R6/2 HD fragment mouse model mitochondrial cristae morphology was abnormal. This was associated with a normal fission/fusion balance. However, there was less OPA1 oligomerisation. These steady state differences suggest that the integrity of mitochondrial cristae is compromised. However, this was not associated with leakage of cytochrome c into the cytosol nor substantial activation of caspase 3.

In our HD fragment mouse model we observed in late stage transgenic animals a higher percentage of cortical and striatal mitochondria with abnormal cristae than in wild-type mice. This agrees with findings in brain biopsies from HD patients, the 3-NP HD rat model, the quinolinic acid treated rat model and HD primary human lymphoblasts, where abnormal mitochondrial cristae structure has been described (Costa 2010, Goebel et al. 1978, Mehrotra et al. 2015, Mormone et al. 2006, Tellet-Nagel 1974). The disruption of the mitochondrial cristae structure could be the result of impaired maintenance of mitochondrial outer and/or inner membrane integrity in which mitochondrial fission and fusion plays an important role (Archer 2014, Wai and Langer 2016). However, mitochondrial size and number were similar in transgenic and wild-type mice, indicating that there was no overt phenotype of increased fission – that would have been associated with smaller mitochondria – or increased fusion – that would have caused elongated mitochondria. The analyses of DRP1 and the mitofusins, the main drivers of fission and fusion, did reveal a lower amount of DRP1 transcripts in cortex and striatum, and higher mitofusin 1 mRNA in striatum of transgenic mice compared to wild-type. While this was associated, at the protein level, with less DRP1 in transgenic cortex total lysate, the amount of DRP1 recruited to mitochondria was similar in transgenic and wild-type mice. Mitochondrial fission is mainly initiated by the recruitment of the cytosolic DRP1 to the outer mitochondrial membrane (Otera et al. 2013). Therefore, despite some differences in total lysate DRP1 in transgenic animals, the similar levels of DRP1 in mitochondria does suggest that there is no increase in fission at least not in late stage transgenic animals. This is consistent with the ultra-structural mitochondrial phenotype data in that we did not find any evidence with our two-dimensional morphological assessments to indicate a disruption in the fission/fusion balance. This differs from studies showing an interaction of mHTT with DRP1 that was reported to increase its activity resulting in increased fragmentation of the mitochondrial network in HD patient fibroblast and myoblast cell cultures (Song et al. 2011), and in HD patient lymphoblasts and primary striatal neurons derived from YAC128 transgenic mice in which DRP1 translocation to mitochondria was associated with increased mitochondrial fragmentation (Costa 2010). In post-mortem HD patient striatum, mitochondria were smaller with an increase in DRP1 protein levels predominantly in late

stage HD (Kim et al. 2010) and an increase in enzymatic DRP1 activity (Shirendeb et al. 2012). It is possible that in dividing cells such as lymphoblasts the demands on fission and fusion are higher so that the effects of mutant huntingtin are greater than in the steady state of our R6/2 post-mitotic striatal and cortical tissues. Therefore, the effects of mHTT on the fission/fusion balance may depend on cell type and stage of differentiation which may explain why we did not see any fission/fusion abnormalities in late-stage R6/2 striatum and cortex. Since the inhibition of DRP1 was shown to reverse a phenotype of mitochondrial fragmentation and improved survival in HD mice suggesting it is worth exploring DRP1 inhibition as a potential treatment in HD (Guo et al. 2013).

Since we had no evidence of a disturbed fission/fusion balance in transgenic mice we subsequently investigated two proteins that are important for the integrity of the inner mitochondrial membrane system. Similar levels of mitofilin at the transcriptome and protein level suggest that mitofilin, an important member of the mitochondrial inner membrane organising system (MINOS) (von der Malsburg et al. 2011, Zerbes et al. 2012a, Zerbes et al. 2012b) may not be a major contributor to the abnormal cristae structure that we observed in transgenic mice. We then turned to OPA1 as the main mitochondrial inner membrane fusion factor. OPA1 plays an important role in cristae remodelling and mitophagy (Ramonet et al. 2013, Sekine and Ichijo 2015, Varanita et al. 2015). The cortex of wild-type mice had less OPA1 mRNA than the striatum. The difference at the transcriptome level was not associated with a difference at the overall OPA1 protein level. However, the protein levels of the long OPA1 isoform relative to the short isoform were lower in cortex compared to striatum. In agreement with other data this argues for potentially higher levels of mitophagy in cortex than striatum (Diedrich et al. 2011), and it is possible that the cortex has an inherently higher turnover of mitochondrial proteins than the striatum.

In transgenic mice OPA1 transcript levels were lower in both cortex and striatum but, in contrast to wild-type mice, this was associated with differences at the protein level. In the cortex of transgenic mice levels of both the short and the long OPA1 isoforms were lower than in wild-type. Nonetheless, the ratio of the long relative to the short isoform was reduced indicating more cleavage of OPA1

(Head et al. 2009). Our data therefore suggest that in the R6/2 mice mutant huntingtin reduces OPA1 gene expression and promotes OPA1 cleavage. Since in transgenic striatum OPA1 isoforms were similar to wild-type this seems to be specific for the cortex of mutant mice. It is possible that the inherently higher mitophagy rate in cortex either increases the cortex's vulnerability to the effects of mutant huntingtin, or is better able to compensate for those effects because it can maintain mitochondrial protein homeostasis better than the striatum. In both cortex and striatum there was a shift of OPA1 oligomers from long to short oligomers. This suggests that in our model the mutant N-terminal huntingtin fragment affects OPA1 oligomerisation independent of OPA1 processing in the context of mitophagy. OPA1 oligomerisation is important for maintaining the integrity of mitochondrial cristae (Frezza et al. 2006, Olichon et al. 2003) and, therefore, abnormal OPA1 oligomerisation in our transgenic mice may contribute to the abnormal cristae structure that we observed on EM.

We next asked if these structural abnormalities affected the cristae's ability to maintain the compartmentalisation of cytochrome c. Reduced OPA1 expression or changes in the OPA1 oligomer composition can affect cristae structure and integrity such that more cytochrome c is released into the cytosol where it can induce apoptosis (Cipolat et al. 2006, Frezza et al. 2006, Olichon et al. 2003). We found similar levels of mitochondrial relative to cytoplasmic cytochrome c in cortex and striatum of our transgenic mice. This does not agree with previous reports in the R6/2 fragment model (Kiechle et al, 2002) which suggested that, indeed, the abnormal cristae morphology and reduced OPA1 oligomerisation that we observed may affect the containment of cytochrome c within mitochondria with subsequent increases in cytosolic cytochrome c levels. Levels of the active form of caspase 3, an important executioner in apoptosis (Fernandes-Alnemri et al. 1994, Nicholson et al. 1995) were increased in transgenic mice. However, the effect was small in accord with the notion that cytochrome c released into the cytosol had only a subtle, if any, effect on the cleavage and therefore activation of caspase 3 and was therefore probably below the threshold for the induction of massive apoptosis. Previous studies have shown that a cytochrome c release below 15% had no effect on the cleavage of caspase 3 (Khodjakov et al. 2004, Scorrano et al. 2002). In addition,

fragmentation of the mitochondrial network may be necessary for the complete release of cytochrome c into the cytosol (Scorrano et al. 2002, Yamaguchi et al. 2008). In our transgenic mice there was no evidence to indicate a disruption of the fission/fusion balance at the phenotypic or protein level even though a three-dimensional assessment of mitochondrial shape could reveal more subtle differences. Our data are therefore consistent with the low levels of apoptosis reported in this model (Dodds et al. 2014, Turmaine et al. 2000, Zhang et al. 2003). In the 3-NP HD model, higher levels of apoptosis have been reported in conjunction with mitochondrial cristae remodeling and increased cytosolic cytochrome c (Mehrotra et al. 2015), and in HD patient lymphoblasts and primary striatal neurons derived from YAC128 transgenic mice OPA1 oligomer disruption and increased sensitivity to apoptosis inducing toxins was another feature (Costa 2010). However, in HD patient caudate nucleus levels of apoptosis and caspase 3, while higher than in controls, were low (Vis et al. 2005). It is possible that the low steady state levels of caspase 3 activation we observed in our transgenic mice may be enhanced sufficiently to cause apoptotic cell death in individual brain cells when mitochondria are stressed. Low levels of cell loss could then accumulate over time. It is also possible that caspase 3 has additional roles in HD such as cleavage of huntingtin (D'Amelio et al. 2012).

Taken together, in cortex and striatum of the late stage HD R6/2 fragment model we observed a phenotype of ultra-structurally abnormal mitochondrial cristae associated with reduced OPA1 oligomerisation. This did not affect the compartmentalisation of cytochrome c consistent with the non-significant low levels of caspase 3 cleavage. This is in good agreement with the low levels of apoptosis that have been reported in this model. Mitochondrial cristae remodelling and cytochrome c release seem a common feature across different HD models including human cell models (Costa and Scorrano 2012, Goebel et al. 1978, Kiechle et al. 2002, Mehrotra et al. 2015, Mormone et al. 2006, Tellet-Nagel 1974). While we do not find evidence for an imbalance of fission and fusion at steady state it is possible that with increased mitochondrial stress mutant huntingtin may promote fission (Jin et al. 2013, Ventura et al. 2012) and further destabilise mitochondrial cristae to promote cytochrome c release sufficient to cause apoptosis. However, it is also possible that there is a fission-

independent mechanism by which mutant huntingtin affects mitochondrial cristae modelling via OPA1 oligomerisation (Cipolat et al. 2006, Frezza et al. 2006, Olichon et al. 2003).

Acknowledgements

We thank the electron microscopy unit (head Prof. Walther) and the animal facilities at Ulm University for their support and CHDI Foundation, Inc., for funding.

Conflict of interest statement

The authors have no conflicts of interest.

Figures

Figure 1. Ultrastructural mitochondrial morphology. A. Transgenic mice (tg) harboured more mitochondria with vacuoles than wild-type (wt). Mitochondria of the cortex showed less cristae in transgenic mice compared to wild-type (magnification x40,000; arrow=mitochondria). **B-D**. Semi-quantitative analysis of ultrastructural mitochondrial morphology. Average area per mitochondrion (**B**), number of mitochondria (**C**), and mitochondrial area per image (**D**) were similar in wild-type and transgenic mice. **E.** The percentage of mitochondria with altered cristae morphology was significantly higher in transgenic mice than wild-type. Data are means and SEM from n=10 animals. Uni-variate analysis of variance (ANOVA *F*-test), * $p < 0.05$, $^{\#}$ $p < 0.05$ main effect of genotype.

Figure 2. Fission and fusion factors. A. mRNA levels (RT-qPCR) of *Drp1* were lower in striatum and cortex of transgenic mice (tg) compared to wild-type (wt). **B, D.** On western blot with corresponding quantification relative to protein stain, DRP1 protein levels were lower in cortex of transgenic mice. **C, D.** Protein levels of DRP1 in enriched mitochondrial fractions relative to the total amount of DRP1 were similar in transgenic and wild-type. **E, F.** mRNA levels (RT-qPCR) of *Mfn1* (E) and *Mfn2* (F) were lower in wild-type cortex compared to striatum. *Mfn1* levels in transgenic striatum were higher than in wild-type. **G-I.** Representative western blot with corresponding quantification relative to protein stain showed reduced MFN2 protein levels in cortex compared to striatum, while MFN1 was similar in both brain regions. DRP1 protein data are log transformed. Data are means (±SEM) from n=8-10 samples. Uni-variate analysis of variance (ANOVA *F*-test), * $p < 0.05$, *** $p < 0.001$, $^{\#}$ $p < 0.05$ main effect of genotype.

Figure 3. The inner mitochondrial membrane protein mitofilin. A. mRNA levels (RT-qPCR) of mitofilin (*Immt)* were similar in transgenic striatum and cortex compared to wild-type. **B, C.** Quantitative western blot analysis of SDS-PAG relative to total protein stain showed that mitofilin (IMMT) levels were similar in cortex and striatum of wild-type and transgenic mice. **D.** Blue native gel electrophoresis followed by western blot analysis of mitofilin protein associations revealed no

differences between wild-type and transgenic tissues. Data are means (±SEM) from n=8-10 animals. Uni-variate analysis of variance (ANOVA *F*-test)

Figure 4. The inner mitochondrial membrane protein OPA1. A. Lower *Opa1* mRNA levels (qPCR) in cortex compared to striatum. Cortex of transgenic mice had less *Opa1* mRNA compared to wild-type. **B, C.** At protein level (western blot) the ratio of the long relative to the short OPA1 isoform was lower in cortex compared to striatum. In cortex of transgenic mice, the long to short OPA1 isoform ratio was lower compared to wild-type cortex. **D, E, F.** Blue native gel electrophoresis and western blot analysis of OPA1 oligomers relative to total protein stain showed an increase of small oligomers of ~300 kDa in striatum of transgenic mice. Data are means (±SEM) from n=8-10 animals. Uni-variate analysis of variance (ANOVA *F*-test), * $p < 0.05$, *** $p < 0.00$; $^{\#}$ $p < 0.05$, $^{\#\#}$ $p < 0.01$ main effect of genotype.

Figure 5. Cytochrome c A. Fractionation leads to a mitochondrial fraction (MF) and a cytosolic fraction (CF). Compared to total lysate (TL) the MF is strongly enriched for mitochondria, while mitochondria are strongly diminished in the CF. B. In separate western blots cytosolic, or mitochondrial, fractions from transgenic (tg) and wild-type (wt) mice contain similar amounts of cytochrome c. HPRT is the loading control for the cytosol, NDUFA9 for mitochondria.

Table1: Primer sequences for qPCR

Name	RefSeq	Primer sequence	Efficiency	Temperature (°C)
Mfn1	NM_024200.4	GCCCTGTCCAGGTGCATAAT	107.5	64.4
		TGGCCGAAGATTGCAGTGAT		
Mfn2	NM_133201.2	GGTCAGGGGTATCAGCGAAG	107.7	64.4
		TTGTCCCAGAGCATGGCATT		
Drp1	NM_152816.2	CCCGGAGACCTCTCATTCTG	95.1	62
		GTCTTGAGTTTTTCCATGTGGC		
Opa1	NM_001199177.1	CAGTTTAGCTCCCGACCTGG	106.9	60
		ACAAGAGAAGGGCCTCAGAAA		
Immt	NM_029673.3	TCAAAAAGGTCCAGGCTGCT	105.8	60
		CCCTTTCCATCCAGGAGTGAT		
Cycs	NM_007808.4	AACGTTCGTGGTGTTGACC	120.8	60
		TTATGCTTGCCTCCCTTTTC		
Poldip3	NM_178627.3	AGGTAGGCTGTGTTTGTCGG	101.5	61.4
		CCAATACGTTCCTGCACCCT		
Metap1	NM_175224.4	TGCGACTCGTGTGTAGGC	102.4	60
		CTTCAGTAGTTACACCCGCTTTAAT		

Supplementary material:

Figure S1. Quantitative OPA1 protein levels. At protein level (western blot) transgenic mice contain less of the short (**A**) and long (**B**) isoform of OPA1 relative to total OPA1 in cortex. **C.** Quantitative western blot analysis relative to total protein stain showed similar levels of OPA1 oligomers of 480 kDa in striatum and cortex of transgenic mice compared to wild-type. Data are means (±SEM) from n=8-10 animals. Uni-variate analysis of variance (ANOVA *F*-test), * $p < 0.05$.

Figure S2. Cytochrome c and Caspase 3. A. mRNA levels (RT-qPCR) of cytochrome c were lower in cortex than in striatum. **B.** At protein level (quantitative western blot) total lysate cytochrome c was lower in cortex than striatum. **C.** At the protein level (western blot) the amount of uncleaved caspase 3 was similar in wild-type and transgenic mice. **D.** Similar levels of caspase 3 cleaved relative to the uncleaved isoform in wild-type and transgenic mice. Data are means (±SEM) from n=8-10 animals. Uni-variate analysis of variance (ANOVA *F*-test).

References

1. Altman D: Analysis of skewed data. In: Practical statistics for medical research. Chapman & Hall, London, 199-205 (1991)

2. Anand R, Wai T, Baker MJ, Kladt N, Schauss AC, Rugarli E, Langer T: The i-AAA protease YME1L and OMA1 cleave OPA1 to balance mitochondrial fusion and fission. The Journal of cell biology 204:919-929.(2014)

3. Archer SL: Mitochondrial fission and fusion in human diseases. The New England journal of medicine 370:1074.(2014)

4. Bereiter-Hahn J, Voth M: Dynamics of mitochondria in living cells: shape changes, dislocations, fusion, and fission of mitochondria. Microscopy research and technique 27:198-219.(1994)

5. Chan DC: Mitochondrial fusion and fission in mammals. Annual review of cell and developmental biology 22:79-99.(2006a)

6. Chan DC: Mitochondria: dynamic organelles in disease, aging, and development. Cell 125:1241-1252.(2006b)

7. Cipolat S, Rudka T, Hartmann D, Costa V, Serneels L, Craessaerts K, Metzger K, Frezza C, Annaert W, D'Adamio L, Derks C, Dejaegere T, Pellegrini L, D'Hooge R, Scorrano L, De Strooper B: Mitochondrial rhomboid PARL regulates cytochrome c release during apoptosis via OPA1-dependent cristae remodeling. Cell 126:163-175.(2006)

8. Costa V: Mitochondrial fission and cristae disruption

increase the response of cell models of

Huntington’s disease to apoptotic stimuli. EMBO Molecular Medecine.(2010)

9. Costa V, Scorrano L: Shaping the role of mitochondria in the pathogenesis of Huntington's disease. The EMBO journal 31:1853-1864.(2012)

10. D'Amelio M, Sheng M, Cecconi F: Caspase-3 in the central nervous system: beyond apoptosis. Trends in neurosciences 35:700-709.(2012)

11. Diedrich M, Kitada T, Nebrich G, Koppelstaetter A, Shen J, Zabel C, Klose J, Mao L: Brain region specific mitophagy capacity could contribute to selective neuronal vulnerability in Parkinson's disease. Proteome science 9:59.(2011)

12. Dodds L, Chen J, Berggren K, Fox J: Characterization of Striatal Neuronal Loss and Atrophy in the R6/2 Mouse Model of Huntington's Disease. PLoS currents 6.(2014)

13. Fernandes-Alnemri T, Litwack G, Alnemri ES: CPP32, a novel human apoptotic protein with homology to Caenorhabditis elegans cell death protein Ced-3 and mammalian interleukin-1 beta-converting enzyme. The Journal of biological chemistry 269:30761-30764.(1994)

14. Frezza C, Cipolat S, Martins de Brito O, Micaroni M, Beznoussenko GV, Rudka T, Bartoli D, Polishuck RS, Danial NN, De Strooper B, Scorrano L: OPA1 controls apoptotic cristae remodeling independently from mitochondrial fusion. Cell 126:177-189.(2006)

15. Goebel HH, Heipertz R, Scholz W, Iqbal K, Tellez-Nagel I: Juvenile Huntington chorea: clinical, ultrastructural, and biochemical studies. Neurology 28:23-31.(1978)

16. Guo X, Disatnik MH, Monbureau M, Shamloo M, Mochly-Rosen D, Qi X: Inhibition of mitochondrial fragmentation diminishes Huntington's disease-associated neurodegeneration. The Journal of clinical investigation 123:5371-5388.(2013)

17. Head B, Griparic L, Amiri M, Gandre-Babbe S, van der Bliek AM: Inducible proteolytic inactivation of OPA1 mediated by the OMA1 protease in mammalian cells. The Journal of cell biology 187:959-966.(2009)

18. Hellemans J, Mortier G, De Paepe A, Speleman F, Vandesompele J: qBase relative quantification framework and software for management and automated analysis of real-time quantitative PCR data. Genome biology 8:R19.(2007)

19. Hering T, Birth N, Taanman JW, Orth M: Selective striatal mtDNA depletion in end-stage Huntington's disease R6/2 mice. Experimental neurology 266C:22-29.(2015)

20. Jin YN, Yu YV, Gundemir S, Jo C, Cui M, Tieu K, Johnson GV: Impaired mitochondrial dynamics and Nrf2 signaling contribute to compromised responses to oxidative stress in striatal cells expressing full-length mutant huntingtin. PloS one 8:e57932.(2013)

21. Khodjakov A, Rieder C, Mannella CA, Kinnally KW: Laser micro-irradiation of mitochondria: is there an amplified mitochondrial death signal in neural cells? Mitochondrion 3:217-227.(2004)

22. Kiechle T, Dedeoglu A, Kubilus J, Kowall NW, Beal MF, Friedlander RM, Hersch SM, Ferrante RJ: Cytochrome C and caspase-9 expression in Huntington's disease. Neuromolecular medicine 1:183-195.(2002)

23. Kim J, Moody JP, Edgerly CK, Bordiuk OL, Cormier K, Smith K, Beal MF, Ferrante RJ: Mitochondrial loss, dysfunction and altered dynamics in Huntington's disease. Human molecular genetics 19:3919-3935.(2010)

24. Kushnareva YE, Gerencser AA, Bossy B, Ju WK, White AD, Waggoner J, Ellisman MH, Perkins G, Bossy-Wetzel E: Loss of OPA1 disturbs cellular calcium homeostasis and sensitizes for excitotoxicity. Cell death and differentiation 20:353-365.(2013)

25. Lin MY, Sheng ZH: Regulation of mitochondrial transport in neurons. Experimental cell research.(2015)

26. Mangiarini L, Sathasivam K, Seller M, Cozens B, Harper A, Hetherington C, Lawton M, Trottier Y, Lehrach H, Davies S, Bates G: Exon 1 of the HD Gene with an Expanded

CAG Repeat Is Sufficient to Cause a Progressive

Neurological Phenotype in Transgenic Mice. Cell 87:493-506.(1996)

27. Mehrotra A, Kanwal A, Banerjee SK, Sandhir R: Mitochondrial modulators in experimental Huntington's disease: reversal of mitochondrial dysfunctions and cognitive deficits. Neurobiology of aging 36:2186-2200.(2015)

28. Mormone E, Matarrese P, Tinari A, Cannella M, Maglione V, Farrace MG, Piacentini M, Frati L, Malorni W, Squitieri F: Genotype-dependent priming to self- and xeno-cannibalism in heterozygous and homozygous lymphoblasts from patients with Huntington's disease. Journal of neurochemistry 98:1090-1099.(2006)

29. Nicholson DW, Ali A, Thornberry NA, Vaillancourt JP, Ding CK, Gallant M, Gareau Y, Griffin PR, Labelle M, Lazebnik YA, et al.: Identification and inhibition of the ICE/CED-3 protease necessary for mammalian apoptosis. Nature 376:37-43.(1995)

30. Olichon A, Baricault L, Gas N, Guillou E, Valette A, Belenguer P, Lenaers G: Loss of OPA1 perturbates the mitochondrial inner membrane structure and integrity, leading to cytochrome c release and apoptosis. The Journal of biological chemistry 278:7743-7746.(2003)

31. Orr AL, Li S, Wang CE, Li H, Wang J, Rong J, Xu X, Mastroberardino PG, Greenamyre JT, Li XJ: N-terminal mutant huntingtin associates with mitochondria and impairs mitochondrial trafficking. The Journal of neuroscience : the official journal of the Society for Neuroscience 28:2783-2792.(2008)

32. Otera H, Ishihara N, Mihara K: New insights into the function and regulation of mitochondrial fission. Biochimica et biophysica acta 1833:1256-1268.(2013)

33. Ramonet D, Perier C, Recasens A, Dehay B, Bove J, Costa V, Scorrano L, Vila M: Optic atrophy 1 mediates mitochondria remodeling and dopaminergic neurodegeneration linked to complex I deficiency. Cell death and differentiation 20:77-85.(2013)

34. Ross CA, Tabrizi SJ: Huntington's disease: from molecular pathogenesis to clinical treatment. The Lancet Neurology 10:83-98.(2011)

35. Ross CA, Aylward EH, Wild EJ, Langbehn DR, Long JD, Warner JH, Scahill RI, Leavitt BR, Stout JC, Paulsen JS, Reilmann R, Unschuld PG, Wexler A, Margolis RL, Tabrizi SJ: Huntington disease: natural history, biomarkers and prospects for therapeutics. Nature reviews Neurology 10:204-216.(2014)

36. Schagger H, von Jagow G: Blue native electrophoresis for isolation of membrane protein complexes in enzymatically active form. Analytical biochemistry 199:223-231.(1991)

37. Scorrano L, Ashiya M, Buttle K, Weiler S, Oakes SA, Mannella CA, Korsmeyer SJ: A distinct pathway remodels mitochondrial cristae and mobilizes cytochrome c during apoptosis. Developmental cell 2:55-67.(2002)

38. Sekine S, Ichijo H: Mitochondrial proteolysis: Its emerging roles in stress responses. Biochimica et biophysica acta 1850:274-280.(2015)

39. Shirendeb UP, Calkins MJ, Manczak M, Anekonda V, Dufour B, McBride JL, Mao P, Reddy PH: Mutant huntingtin's interaction with mitochondrial protein Drp1 impairs mitochondrial biogenesis and causes defective axonal transport and synaptic degeneration in Huntington's disease. Human molecular genetics 21:406-420.(2012)

40. Song W, Chen J, Petrilli A, Liot G, Klinglmayr E, Zhou Y, Poquiz P, Tjong J, Pouladi MA, Hayden MR, Masliah E, Ellisman M, Rouiller I, Schwarzenbacher R, Bossy B, Perkins G, Bossy-Wetzel E: Mutant huntingtin binds the mitochondrial fission GTPase dynamin-related protein-1 and increases its enzymatic activity. Nature medicine 17:377-382.(2011)

41. Tellet-Nagel: Studies on brain biopsies of patients with Huntington`s chorea.(1974)

42. The Huntington's Disease Collaborative Research Group X: A novel gene containing a trinucleotide repeat that is expanded and unstable on Huntington's disease chromosomes. The Huntington's Disease Collaborative Research Group. Cell 72:971-983.(1993)

43. Turmaine M, Raza A, Mahal A, Mangiarini L, Bates GP, Davies SW: Nonapoptotic neurodegeneration in a transgenic mouse model of Huntington's disease. Proceedings of the National Academy of Sciences of the United States of America 97:8093-8097.(2000)

44. Twing G: Fission and selective fusion govern mitochondrial

segregation and elimination by autophagy. The EMBO journal 27:433-446.(2008)

45. Varanita T, Soriano ME, Romanello V, Zaglia T, Quintana-Cabrera R, Semenzato M, Menabo R, Costa V, Civiletto G, Pesce P, Viscomi C, Zeviani M, Di Lisa F, Mongillo M, Sandri M, Scorrano L: The OPA1-dependent mitochondrial cristae remodeling pathway controls atrophic, apoptotic, and ischemic tissue damage. Cell metabolism 21:834-844.(2015)

46. Ventura I, Russo MT, De Nuccio C, De Luca G, Degan P, Bernardo A, Visentin S, Minghetti L, Bignami M: hMTH1 expression protects mitochondria from Huntington's disease-like impairment. Neurobiology of disease 49C:148-158.(2012)

47. Vis JC, Schipper E, de Boer-van Huizen RT, Verbeek MM, de Waal RM, Wesseling P, ten Donkelaar HJ, Kremer B: Expression pattern of apoptosis-related markers in Huntington's disease. Acta neuropathologica 109:321-328.(2005)

48. von der Malsburg K, Muller JM, Bohnert M, Oeljeklaus S, Kwiatkowska P, Becker T, Loniewska-Lwowska A, Wiese S, Rao S, Milenkovic D, Hutu DP, Zerbes RM, Schulze-Specking A, Meyer HE, Martinou JC, Rospert S, Rehling P, Meisinger C, Veenhuis M, Warscheid B, van der Klei IJ, Pfanner N, Chacinska A, van der Laan M: Dual role of mitofilin in mitochondrial membrane organization and protein biogenesis. Developmental cell 21:694-707.(2011)

49. Wai T, Langer T: Mitochondrial Dynamics and Metabolic Regulation. Trends in endocrinology and metabolism: TEM 27:105-117.(2016)

50. Westermann B: Mitochondrial fusion and fission in cell life and death. Nature reviews Molecular cell biology 11:872-884.(2010)

51. Yamaguchi R, Lartigue L, Perkins G, Scott RT, Dixit A, Kushnareva Y, Kuwana T, Ellisman MH, Newmeyer DD: Opa1-mediated cristae opening is Bax/Bak and BH3 dependent, required for apoptosis, and independent of Bak oligomerization. Molecular cell 31:557-569.(2008)

52. Yano H, Baranov SV, Baranova OV, Kim J, Pan Y, Yablonska S, Carlisle DL, Ferrante RJ, Kim AH, Friedlander RM: Inhibition of mitochondrial protein import by mutant huntingtin. Nature neuroscience 17:822-831.(2014)

53. Youle RJ, van der Bliek AM: Mitochondrial fission, fusion, and stress. Science 337:1062-1065.(2012)

54. Zerbes RM, Bohnert M, Stroud DA, von der Malsburg K, Kram A, Oeljeklaus S, Warscheid B, Becker T, Wiedemann N, Veenhuis M, van der Klei IJ, Pfanner N, van der Laan M: Role of MINOS in mitochondrial membrane architecture: cristae morphology and outer membrane interactions differentially depend on mitofilin domains. Journal of molecular biology 422:183-191.(2012a)

55. Zerbes RM, van der Klei IJ, Veenhuis M, Pfanner N, van der Laan M, Bohnert M: Mitofilin complexes: conserved organizers of mitochondrial membrane architecture. Biological chemistry 393:1247-1261.(2012b)

56. Zhang Y, Ona VO, Li M, Drozda M, Dubois-Dauphin M, Przedborski S, Ferrante RJ, Friedlander RM: Sequential activation of individual caspases, and of alterations in Bcl-2 proapoptotic signals in a mouse model of Huntington's disease. Journal of neurochemistry 87:1184-1192.(2003)

Figures

Fig. 1

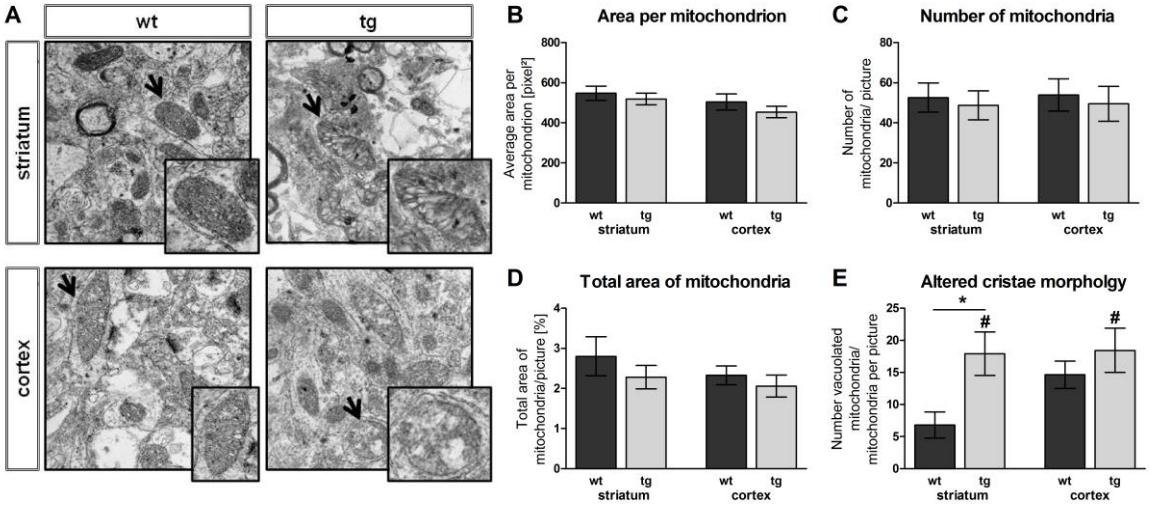

Fig. 2

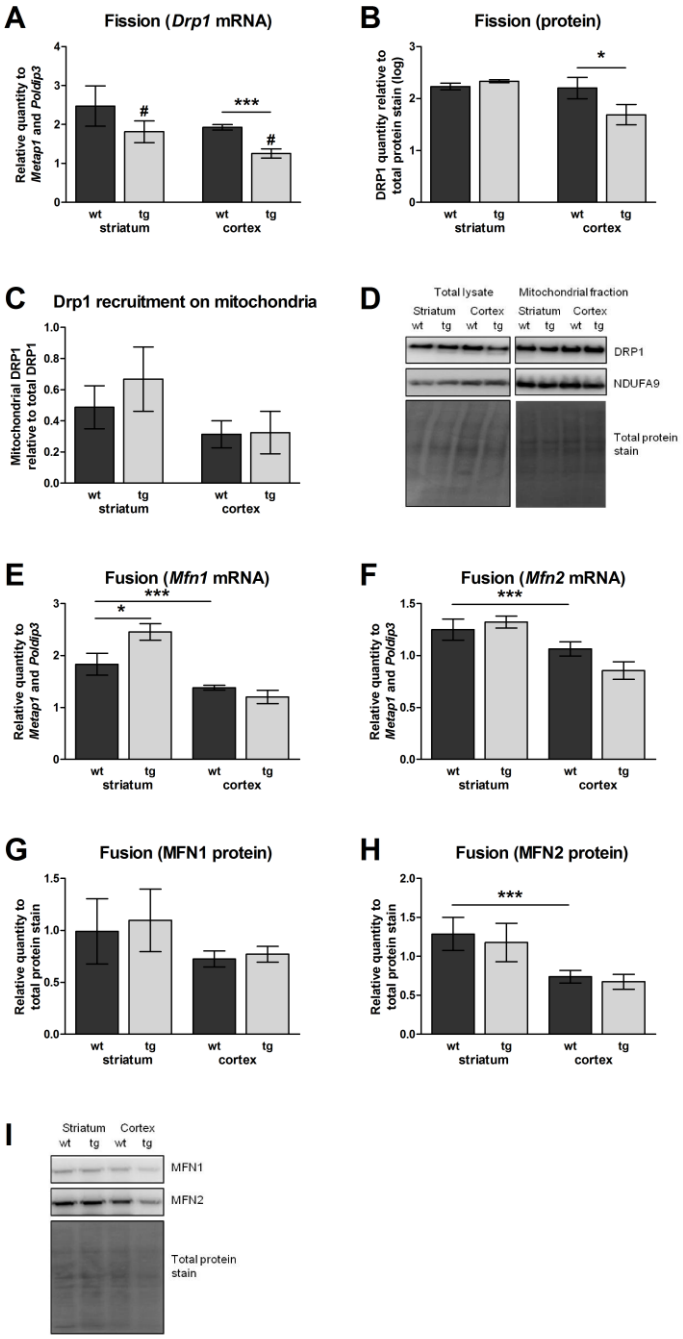
A
Fission (Drp1 mRNA)
Relative quantity to Metap1 and Poldip3
wt tg wt tg
striatum cortex
B
Fission (protein)
DRP1 quantity relative to total protein stain (log)
C
Drp1 recruitment on mitochondria
Mitochondrial DRP1 relative to total DRP1
D
Total lysate
Mitochondrial fraction
Striatum Cortex Striatum Cortex
DRP1
NDUFA9
Total protein stain
E
Fusion (Mfn1 mRNA)
F
Fusion (Mfn2 mRNA)
G
Fusion (MFN1 protein)
Relative quantity to total protein stain
H
Fusion (MFN2 protein)
I
MFN1
MFN2
Total protein stain

Fig. 3

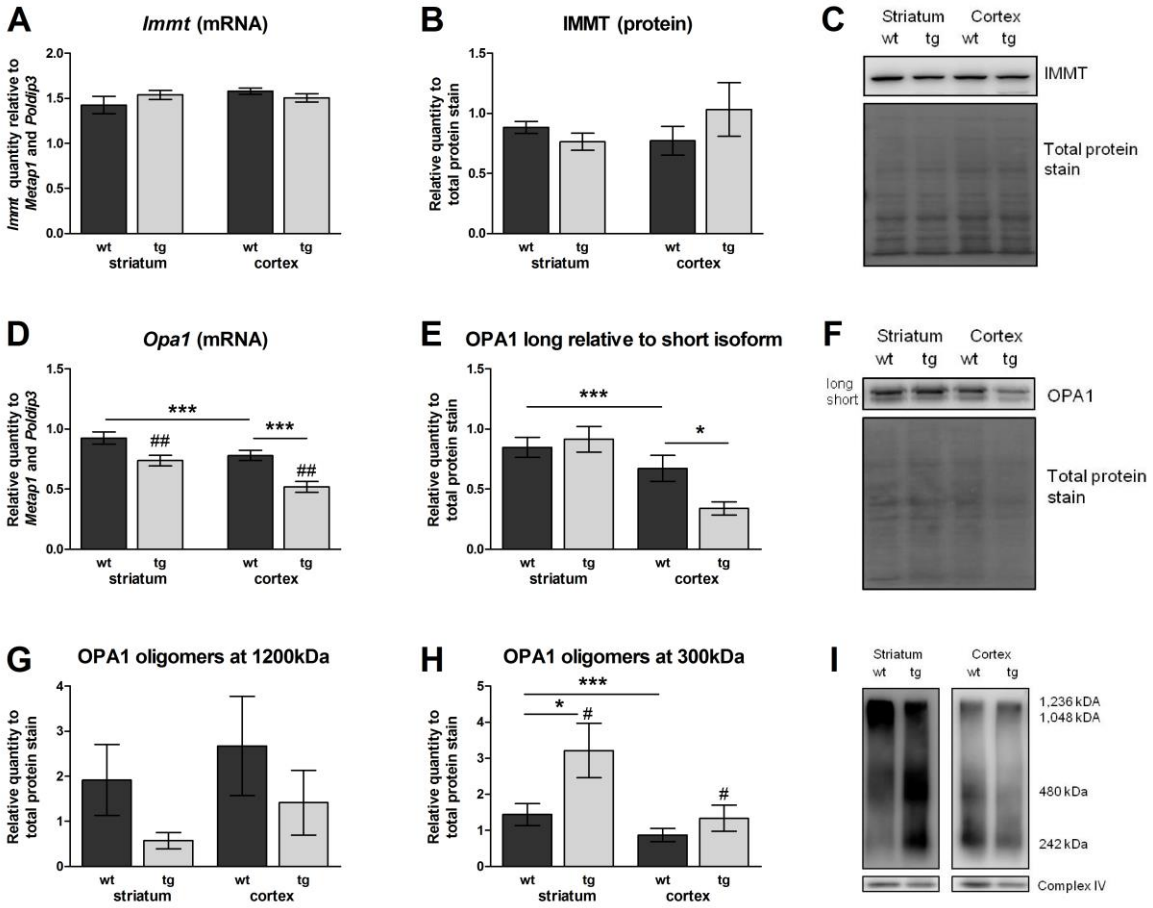
A
Immt (mRNA)
Immt quantity relative to Metap1 and Poldip3
wt tg wt tg
striatum cortex
B
IMMT (protein)
Relative quantity to total protein stain
C
Striatum Cortex
wt tg wt tg
IMMT
Total protein stain
D
Opa1 (mRNA)
Relative quantity to Metap1 and Poldip3
***
***
##
##
E
OPA1 long relative to short isoform
Relative quantity to total protein stain
***
*
F
long short
OPA1
Total protein stain
G
OPA1 oligomers at 1200kDa
Relative quantity to total protein stain
H
OPA1 oligomers at 300kDa
***
*
#
#
I
1,236 kDA
1,048 kDA
480 kDa
242 kDa
Complex IV

Fig. 4

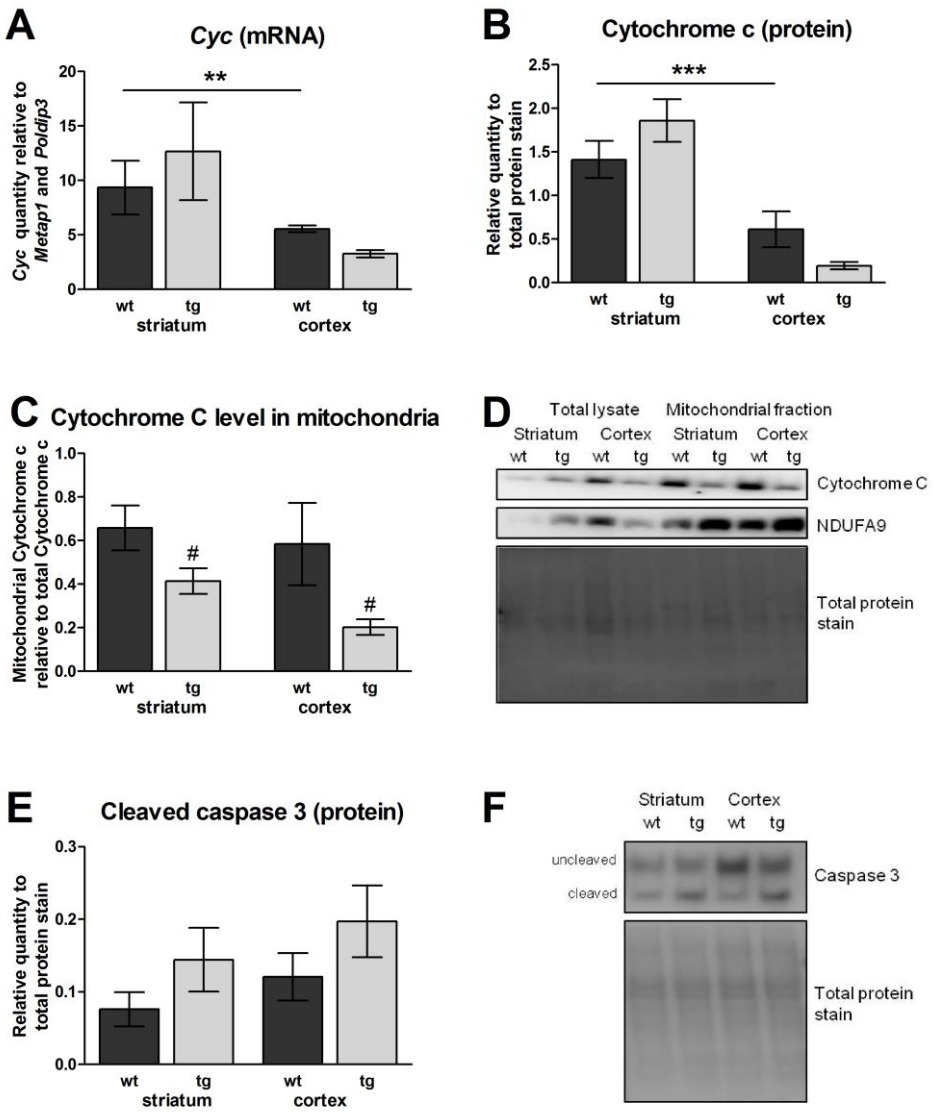
A
Cyc (mRNA)
Cyc quantity relative to Metap1 and Poldip3
**
wt tg wt tg
striatum cortex
B
Cytochrome c (protein)
Relative quantity to total protein stain
***
wt tg wt tg
striatum cortex
C
Cytochrome C level in mitochondria
Mitochondrial Cytochrome c relative to total Cytochrome c
#
#
wt tg wt tg
striatum cortex
D
Total lysate
Mitochondrial fraction
Striatum Cortex Striatum Cortex
wt tg wt tg wt tg wt tg
Cytochrome C
NDUFA9
Total protein stain
E
Cleaved caspase 3 (protein)
Relative quantity to total protein stain
wt tg wt tg
striatum cortex
F
Striatum Cortex
wt tg wt tg
uncleaved
cleaved
Caspase 3
Total protein stain

Supplementary material:

Fig. S1

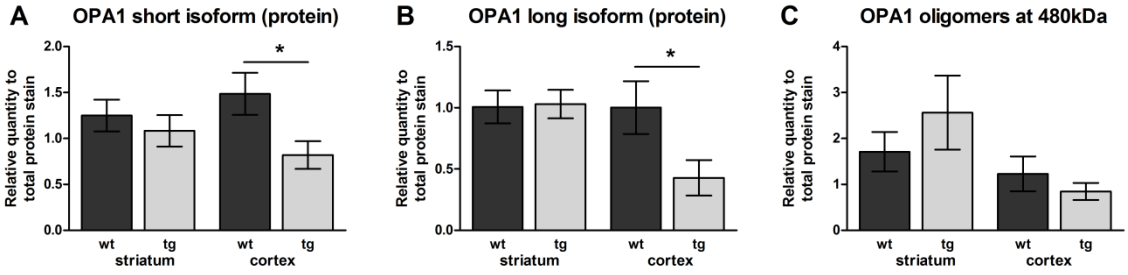

Fig. S2